

# Ordinal Synchronization and Typical States in High-Frequency Digital Markets

M. López<sup>1,\*</sup>, R. Mansilla<sup>2</sup>

<sup>1</sup>Facultad de Ciencias, Universidad Nacional Autónoma de México,  
Ciudad Universitaria, 04510, Ciudad de México, México.

<sup>2</sup>Centro de Investigaciones Interdisciplinarias en Ciencias y Humanidades,  
Universidad Nacional Autónoma de México, Ciudad Universitaria, 04510, Ciudad de México, México.

\* Correspondence: mariolopper@gmail.com

## Abstract

In this paper we show, through the study of ordinal patterns, information theoretic and network measures and clustering algorithms, the presence of typical states in automated high-frequency records during a one-year period in the US stock market, characterized by their degree of centralized or decentralized synchronicity. We also find two whole coherent seasons of highly centralized and decentralized synchronicity, respectively.

**Keywords**— Ordinal Patterns, High-Frequency Trading, Algorithmic Trading, Networks, Synchronicity, Clustering

## 1 Introduction

Financial markets are highly complex evolving systems, which means that their statistical dynamics change in time and are defined by the interaction of economic agents. Thus, it is not surprising that, in order to understand these dynamics, much effort have been recently dedicated to study them as dynamical networks which can be analyzed and classified, either topologically to quantify crisis periods [1] [2] or by clustering them to detect market states [3][4] [5] [6] [7] and possibly early precursors for the catastrophic ones [8] [9].

That approach looks very promising for studying Algorithmic High-Frequency Trading, whose rising during the last decades was recently shown to display an even higher degree of networked structure and complexity than those of traditional markets [10]. However, those network-based studies have been carried out mainly by defining edge weights through correlation matrices, which amounts to ignore non-linear interactions (see [11] for an exception, which does not use cluster analysis, but Machine Learning technics). This is not adequate for high-frequency data, normally expected to be very noisy and highly non-linear and non-stationary. Thus, in order to successfully apply the same network-clustering pipeline of those previous works and, at the same time, be able to detect locally complex non-linear interactions, we define dynamical networks of stocks by means of their transcript synchronicity, a measure of pairwise coupling of time series defined through ordinal patterns, a tool which has been successfully applied to discern non-linear deterministic and stochastic dynamics in real-world data [12].

We also propose suitable phase representation spaces for our dynamical network in order to detect meaningful states dynamics through a couple of clustering algorithms. This allows us to detect two whole coherent and quantitatively distinguishable seasons, characterized by their degree of centralized/decentralized synchronicity.

The paper is organized as follows: Section 2 introduces the theoretical background necessary to apply ordinal pattern analysis. Section 3 describes the characteristics of the data. In Section 4 we apply the previously defined measures to individual stocks, in order to detect anomalous behaviors. Section 5 contains the definition of our transcript synchronicity coefficient, which we use to define our dynamical network and discuss the more convenient phase representation spaces for the sake of our analysis. In Section 6 we carry out the clustering analysis to detect typical market states, which in Section 7 are modeled as first order Markov processes. Section 8 contains the conclusions.

## 2 Theoretical Background: Ordinal Patterns

Permutation entropy was introduced in [13] as a (non-parametric) complexity measure, robust to dynamical noise, invariant with respect to nonlinear monotonous transformation and computationally efficient. It is defined as follows: First, given a time series  $x_n$  for  $n = 1, \dots, N$  and  $m < N$ , we consider,  $S_m$ , the group of permutations of length  $m$  and, for  $0 < t \leq N - m + 1$ , we say that the sliding window  $x_m(t) = (x_t, x_{t+1}, \dots, x_{t+m-1})$  is of type  $\pi_t \in S_m$  if  $\pi_t = (i_1, \dots, i_m)$  is the only  $m$ -permutation satisfying the following conditions:

- (1)  $x_{t+i_s} \leq x_{t+i_{s+1}}$  for  $s = 1, \dots, m - 1$ , and
- (2)  $i_s < i_{s+1}$  if  $x_{t+i_s} = x_{t+i_{s+1}}$ ,

and we denote this with  $\Phi(x_m(t)) = \pi_t$ .

The study of this new ordinal patterns series  $\{\pi_t\}_{t < N-m+1}$ , has been applied to biomedicine [14] [15] [16] [17]

[18] [19] [20] [21], paleoclimatology [22], economics [23] [24] [25] [26] [27] [28], geology [29] and engineering [30] for classification and prediction of deterministic and stochastic non-linear dynamics.

So, for any  $\pi \in S_m$  it's relative frequency is defined as:

$$p_m(\pi) = \frac{\#\{t | t \leq N - m + 1, \Phi(x_m(t)) = \pi\}}{N - m + 1}.$$

Although the original proposal by Bandt and Pompe consisted basically in the study of time series through Shannon entropy of the ordinal patterns distribution, called *permutation entropy* (PE) and given by

$$\text{PE}(m) = - \sum_{\pi \in S_m} p_m(\pi) \log p_m(\pi),$$

a vast stream of theoretical and methodological approaches has developed since then, giving place to a constellation of complexity measures, important examples of which are weighted permutation entropy [31] [32], symbolic transfer entropy [33] [34], statistical complexity [26] [35] [36], various measures of coupling and synchronicity [20] [37][34] [38] and network-based measures [29] (we will define some of them below). Other studies had combined these analytical tools with Machine Learning technics [16] [39], and still others had exploited the algebraic structure of  $S_m$  [38] [40] [41] [34].

We must be very careful in applying permutation entropy, the authors of [42] warn us. The presence of equal consecutive values in the original time series, which is frequently dealt with by preserving the temporal order in the corresponding permutation, could lead to draw false conclusions by detecting spurious patters. To adress this issue one can sum low amplitude noise to the original series in order to (randomly) break equalities, as proposed in [43], and that is exactly what we do in this work, with an artificially generated uniform distribution series of amplitude  $10^{-7}$ .

We will need some definitions for the next sections. Given two probability distributions  $p, q$  defined on a finite set, we define its Jensen-Shannon divergence as

$$D_{\text{JS}}(p, q) = \frac{D_{\text{KL}}(p \| M) + D_{\text{KL}}(q \| M)}{2},$$

where  $M = (p + q)/2$  and  $D_{\text{KL}}$  is the Kullback-Leiber divergence:

$$D_{\text{KL}}(p \| q) = \sum_i p_i \log \frac{p_i}{q_i},$$

or the relative entropy from  $q$  to  $p$ , of which  $D_{\text{JS}}$  is thus a smoothed, symmetric version.

So, if  $p_m$  is the probability distribution of ordinal patterns of the time series  $x_i$ , we define its *statistical complexity* (Com) [26] [35] [36] as

$$\text{Com}(p_m) = D_{\text{JS}}(p_m, u_m) H(p_m),$$

where  $u_m$  is the uniform distribution on  $S_m$  and  $H(\cdot)$  is Shannon entropy. Thus, Com aims to measure complexity through a trade-off between randomness and determinism: while Shannon entropy increases as  $p_m$  aparts away from determinism towards randomness, reaching a maximum for  $u_m$ , its divergence from  $u_m$  grows as  $p_m$  aparts away from randomness. PE and Com have been jointly used to classify dynamical regimes [26].

Missing Patterns Frequency (MPF) [44] is defined as

$$\text{MPF}(p_m) = \frac{\#\{\pi \in S_m \mid p_m(\pi) = 0\}}{m!}.$$

As deterministic dynamics are expected to display a relatively small set of ordinal patterns in contrast to random dynamics [44] [24] [25], MPF is understood to quantify determinism degrees.

Yet another methodology for studying ordinal patterns, this time as nodes of a network, has been proposed in [45][46] [47] [29], where the directed edges are weighted according to the transition probability of passing from one pattern to another inmediately in time, thus taking patterns as states of the process. So, for the ordinal sequence  $\{\pi_t\}_{t < N-m+1}$  we define nodes as the ordinal patterns and the weight of their edges are given by the transition probabilities  $p_m(\pi' \mid \pi)$  of observing for some  $t$  that  $\pi_{t+m} = \pi'$  given that  $\pi_t = \pi$ . We can then compute the node entropy as

$$\text{NE}(\pi) = - \sum_{\pi' \in S_m} p_m(\pi' \mid \pi) \log(p_m(\pi' \mid \pi)).$$

These measures, unlike the previously defined, aim to quantify determinism not in terms of pattern frequency, but of pattern transitions in time. Minimum Node Entropy (MNE) and Global Node Entropy (GNE) are defined as [48]

$$\text{MNE}(p_m) = \min\{\text{NE}(\pi) \mid \pi \in S_m\} \text{ and } \text{GNE} = \sum_{\pi \in S_m} p_m(\pi) \text{NE}(\pi),$$

respectively, so MNE measures how deterministic can a pattern be in a given network, while GNE gives us a global, weighted score of pattern transitions determinism. Finally, missing transitions frequency (MTF) is defined as

$$\text{MTF}(p_m) = \frac{\#\{(\pi, \pi') \in S_m \times S_m \mid p_m(\pi' \mid \pi) = 0\}}{(m!)^2},$$

and is of course the analogous measure of MPF for pattern transitions.

A classification plane is proposed in [48], whose axes are given by GNE and the MNE, both of them measured using non-overlapping ordinal patterns to avoid transition constrains. This methodology seems to be very useful, not to mention intuitive, to distinguish between (linear) stochastic and (non-linear) deterministic dynamics. When applied to stock market time series, this methodology allows the authors to discriminate financial dynamics from fractional gaussian noise, since financial scores lie below the diagonal around which the noises cluster.

### 3 Data

The data used in this investigation are the time series of prices of the automated (algorithmic) operations that occurred from March 7, 2018 to March 7, 2019 in the and US market, with a total of 251 trading days and 539,834,024 records.

The importance for this work that the data comes from fully automated transactions cannot be overstated: it is for this alone that we are able to test synchronicity specifically for digital markets.

	Market Code	Name
1	ABT	Abbott Laboratories
2	BAC	Bank of America Corporation
3	BMJ	Bristol-Myers Squibb Company
4	C	Citigroup Inc.
5	CSCO	Cisco Systems, Inc.
6	F	Ford Motor Company
7	FB	Facebook, Inc.
8	FOXA	Twenty-First Century Fox, Inc.
9	GE	General Electric Company
10	GM	General Motors Company
11	HPQ	HP Inc.
12	INTC	Intel Corporation
13	KO	The Coca-Cola Company
14	MDLZ	Mondelez International, Inc.
15	MO	Altria Group, Inc.
16	MS	Morgan Stanley
17	MSFT	Microsoft Corporation
18	ORCL	Oracle Corporation
19	PFE	Pfizer Inc.
20	T	AT&T Inc.
21	TWTR	Twitter, Inc.
22	USB	U.S. Bancorp
23	VZ	Verizon Communication, Inc.
24	WFC	Wells Fargo & Company

Figure 1: Codes and Names of the Studied Assets

The data belongs to 24 assets from the US market: ABT, BAC, BMJ, C, CSCO, F, FB, FOXA, GE, GM, HPQ, INTC, KO, MDLZ, MO, MS, MSFT, ORCL, PFE, TWTR, T, USB, WFC, VZ. The details can be seen in figure 1.

The following analysis are carried out for the series of logarithmic returns

$$r(t, \tau) = x(t + 1, \tau) - x(t, \tau),$$

where  $x(t, \tau)$  is the  $t$ -th term of the series of means of  $\tau$  seconds of logarithms of the prices of a given asset. In this work, we use  $\tau = 5$  and study daily subseries to analyze daily dynamics throughout the year.

## 4 Individual Analysis of Stocks through Ordinal Patterns

For the daily series of five seconds average logarithmic returns of each stock, we calculate PE, Com, MPF, MNE, GNE and MTF (the last three without overlapping patterns, just as in [48]) with  $m = 5$ , that is, we study 5-length ordinal patterns of daily series of returns of 5-seconds averages of logarithms of prices. The choice for  $m$  is dictated by considerations about statistical reliability and the problem of undersampling for PE, Com and MPF [49] [22] (although the same problem remains for MNE, GNE and MTF [48], we keep  $m = 5$  for the sake of a better visualization). Next, we plot the evolution of such quantities along the year, as well as the minimum node entropy vs global node entropy plane.

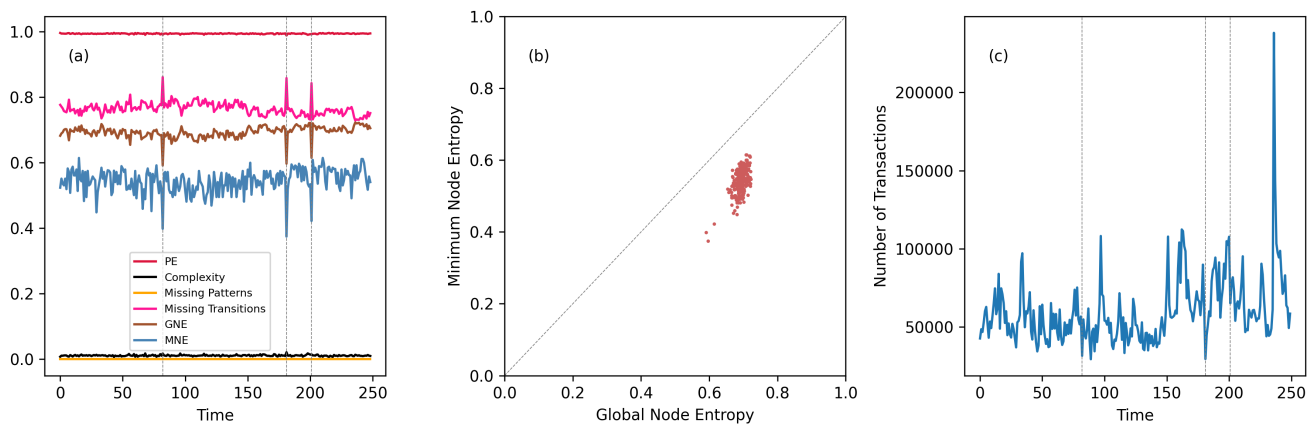


Figure 2: Ordinal Entropy Measures for KO. (a) Permutation Entropy, Complexity, Missing Pattern Frequency, Missing Transition Frequency, Global Node Entropy, Minimum Node Entropy; (b) Minimum Node Entropy vs Global Node Entropy plane; (c) Daily number of transactions.

For the vast majority of stocks, MNE, GNE and MTF clearly present an unusual (outlier) behavior for the days 82, 181 and 201, which we will call outlier days, while we will refer to the other days as typical (figure 2 shows this for KO; outlier days are indicated by vertical gray lines in the left and right panels). These measures abruptly decrease for the outlier days, thus supporting the idea that these days present complex, semi-deterministic behavior: given a certain pattern, the transition to the next one has candidates much more probable than others. In some of the stocks we can further visualize what appears to be a small number of discrete levels for MNE (see second panel in figure 3 for an example). This suggests the existence of a finite number of typical market states, each corresponding to a specific level of MNE. The problem with these measures is that they need length series

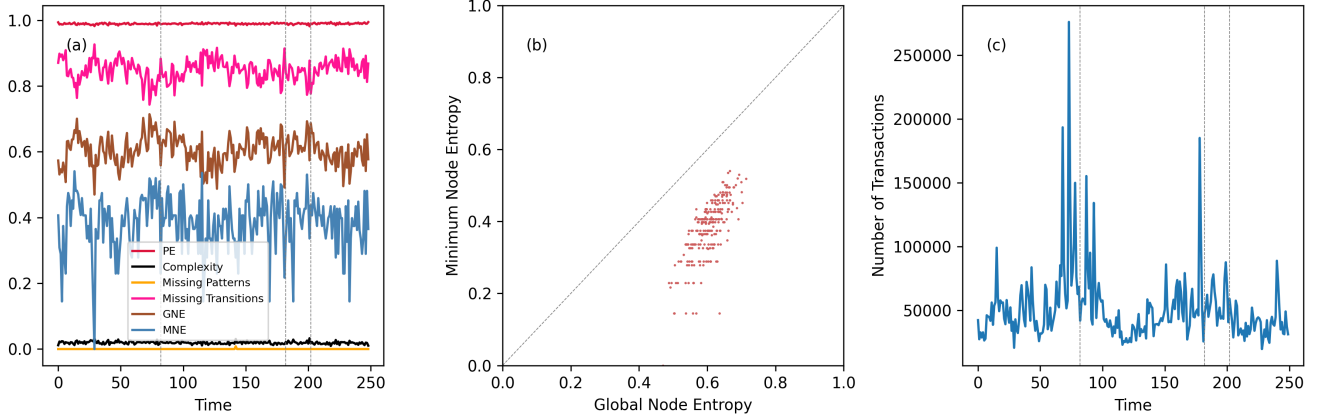


Figure 3: Ordinal Entropy Measures for FOXA. (a) Permutation Entropy, Complexity, Missing Pattern Frequency, Missing Transition Frequency, Global Node Entropy, Minimum Node Entropy; (b) Minimum Node Entropy vs Global Node Entropy plane; (c) Daily number of transactions.

$n \gg (m!)^2$ , and, as already mentioned, we could be undersampling for  $m = 5$ , when we begin to classify outlier days. PE, Com, WPE and MPF are not capable of detecting (visually at least) the outlier days.

By inspecting in the same figure the graphs of the daily number of transactions of each stock (right panel), we can notice that the first two outlier days are low-liquidity days for many of them, although not necessarily global minima or even specially severe drops in some others, while the last outlier does not present this behavior. Thus, low liquidity is not enough to explain this phenomenon.

## 5 Collective Analysis of Stocks through Transcript Synchronicity Dynamical Networks

To get a deeper insight on this behavior and figure out if it is, as it seems to be, a collective behavior, we study the synchronization index given by the transcript entropy of pairs of stocks, that is: for each pair  $(i, j)$  of stocks and each trading day  $T$ , we obtain their daily ordinal pattern sequences  $(\pi_i(t))_{t=1}^n$  and  $(\pi_j(t))_{t=1}^n$  to obtain the transcript series [38] as  $\tau_{i,j}(t) = \pi_j(t) \circ \pi_i(t)^{-1}$ , where the product and the inverse are those of the permutation group  $S_m$ : for  $\pi, \rho \in S_m$ ,  $\pi = (\pi_1, \dots, \pi_m)$  and  $\rho = (\rho_1, \dots, \rho_m)$ ,

$$\pi \circ \rho = (\pi_{\rho_1}, \dots, \pi_{\rho_m}), \text{ and}$$

$$\pi^{-1} : \pi_k \rightarrow k \text{ for } k < m$$

is the sorting operation. In this way, the transcript  $\tau_{i,j}(t)$  is the result of ordering  $\pi_j(t)$  according to the ordinal type of  $\pi_i(t)$ . We take the normalized entropy of this transcript series  $H_T^{transcript}(i, j)$  (that is, the usual permutation entropy of this transcript series) as a (daily) coefficient of desynchronization, and one minus that quantity as our measure of synchronization, which we will call transcript synchronization. Transcript synchronization measures the diversity of transcripts: low transcript synchronization means high variety of transcripts, that is, a lot of different transcripts and then a lot of information is needed to deduce the (ordinal) dynamics of one series given complete knowledge of the other, and analogously for high transcript synchronization. Transcripts have been applied to study synchronization in time series in [40], [41], [50], [34].

Thus we obtain for each trading day a (symmetric) transcript synchronization matrix  $H_T^{transcript}$  of dimension  $n_{stock} \times n_{stock}$  whose  $ij$  value is the transcript synchronization of stocks  $i$  and  $j$  during day  $T$ . By considering each of these daily matrices as adjacency matrices, we obtain a dynamical weighted network through the year, the nodes of which are the stocks and the weight of whose edges are given by our transcript synchronization coefficient. We can thus analyze our time series with classical network-based measures, following [3] [4] [5] [9] [6] [1] [8] [7], which have done that for correlation matrices, and [11], where mutual information networks are studied. We consider two well known such network measures here: degree and eigenvector centrality.

Given a stock labeled as  $i$  and a trading day  $T$ , we define its degree as

$$\text{Degree}(i, T) = \frac{1}{C} \sum_{j=1, j \neq i}^{n_{stocks}} H_T^{transcript}(i, j),$$

so the degree of a node is just the sum of its transcript synchronization with all the other stocks and the normalizing constant  $C$  is such that  $\sum_i \text{Degree}(i, T) = 1$ , while its eigenvector centrality is defined as the  $i$ -th component of the normalized solution to the equation

$$\text{EVC}(i, T) = \frac{1}{\lambda} \sum_{j=1}^{n_{stocks}} H_T^{transcript}(i, j) \text{EVC}(j, T),$$

where  $\lambda$  is the largest eigenvalue of the adjacency matrix  $H_T^{transcript}$ . This is equivalent to find the normalized eigenvector with positive components corresponding to  $\lambda$ , which is known to exist by the Frobenius Theorem. So for each trading day  $T$  we have Degree and EVC, two  $n_{stocks}$ -dimensional vectors widely applied as measures of the importance, centrality or connectedness of a node in the network.

In what follows we remove the first day of the year, for it turns out to be a very peculiar outlier. If we plot the evolution of the histograms of Degree and EVC (figure 4) we can observe a very important increment in the mode of Degree (this will be much more clear in figure 5) during the outlier days and further detect not just those three days, but what appears as two complete consecutive, although intermitent, regimes of highly centralized and decentralized connectivity, the latter weakly present at the beginning of the year and again with much more persistence roughly from day 150 to day 210, and the former just between those periods, approximately from day 50 to day 150. Thus, our outlier days seem to be an extreme manifestation of these collective dynamics. Recall that

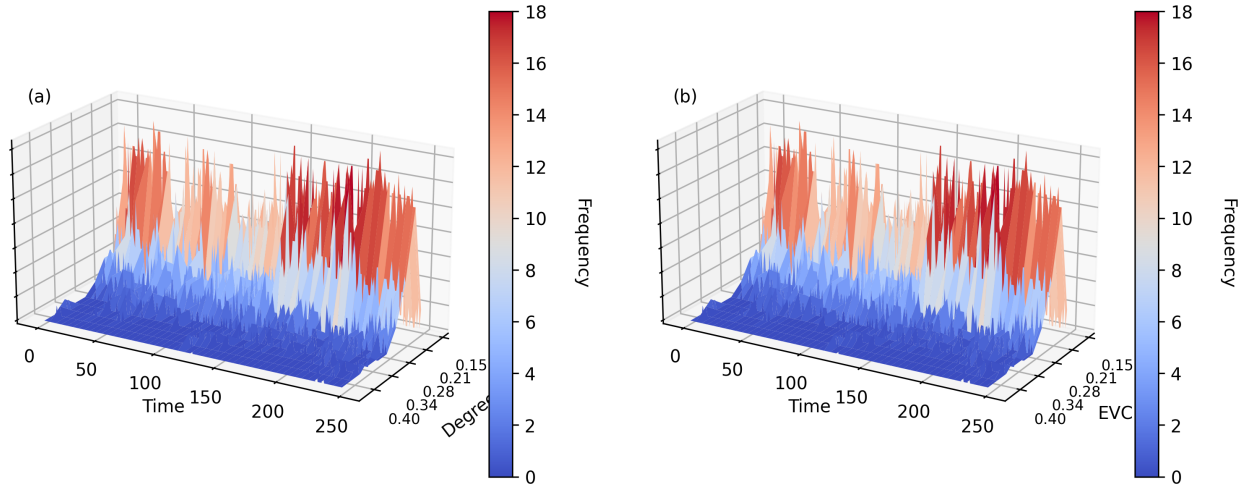


Figure 4: Evolution Through the Trading Year of Histograms of (a) Degree and (b) Eigenvector Centrality for Transcript Synchronization Dynamical Network.

the detection of outlier days and different states at this collective level was by no means an obvious thing to expect, since the only measures capable of detecting them in the individual level were those measuring transitions between consecutive ordinal patterns, while our transcript synchronization coefficient focuses only in simultaneous pairs of patterns across the market.

To further illustrate this behavior, in figures 5 and 6 we plot mean, standard deviation, minimum value and maximum frequency of the previously plotted daily histograms. First of all, for Degree one can easily confirm the presence of the outlier days, as its mean and minimum abruptly increase. Also, and this holds for both figures, at the beginning of the year (March) and during the highly decentralized season we can observe that the mean of the distributions of EVC and Degree increases, while standard deviation decrease, that is to say, the histograms shrink.

Recall that here highly decentralized synchronization means a more uniform distribution of degree-eigenvector centrality among stocks, that is, most of the nodes are equally important in the network. That's why high connectedness can be associated with the shrinking of histograms, in opposition to centralized synchronicity, which happens when there are clearly dominating stocks, much more centrals to the network than the others.

Also in the evolution of Degree and EVC per stock (figure 7), we can see a different regime in about the same period, when their values seem to be distributed more uniformly between stocks than before: both high and low scored stocks tend to equalize each other towards a intermediate value (in the heat graph, blues and reds moves towards white). An exceptional stock, that seems to remain very central to the network through the entire year but with particular orce during the highly centralized season is Citigroup (C). The next stock in importance seems to be Morgan stanley (MS), also from the Financial sector. Interestingly, Facebook (FB) and U. S. Bancorp (USB) increase their influential score just the day after the last two oulier days. Degree very clearly shows again the

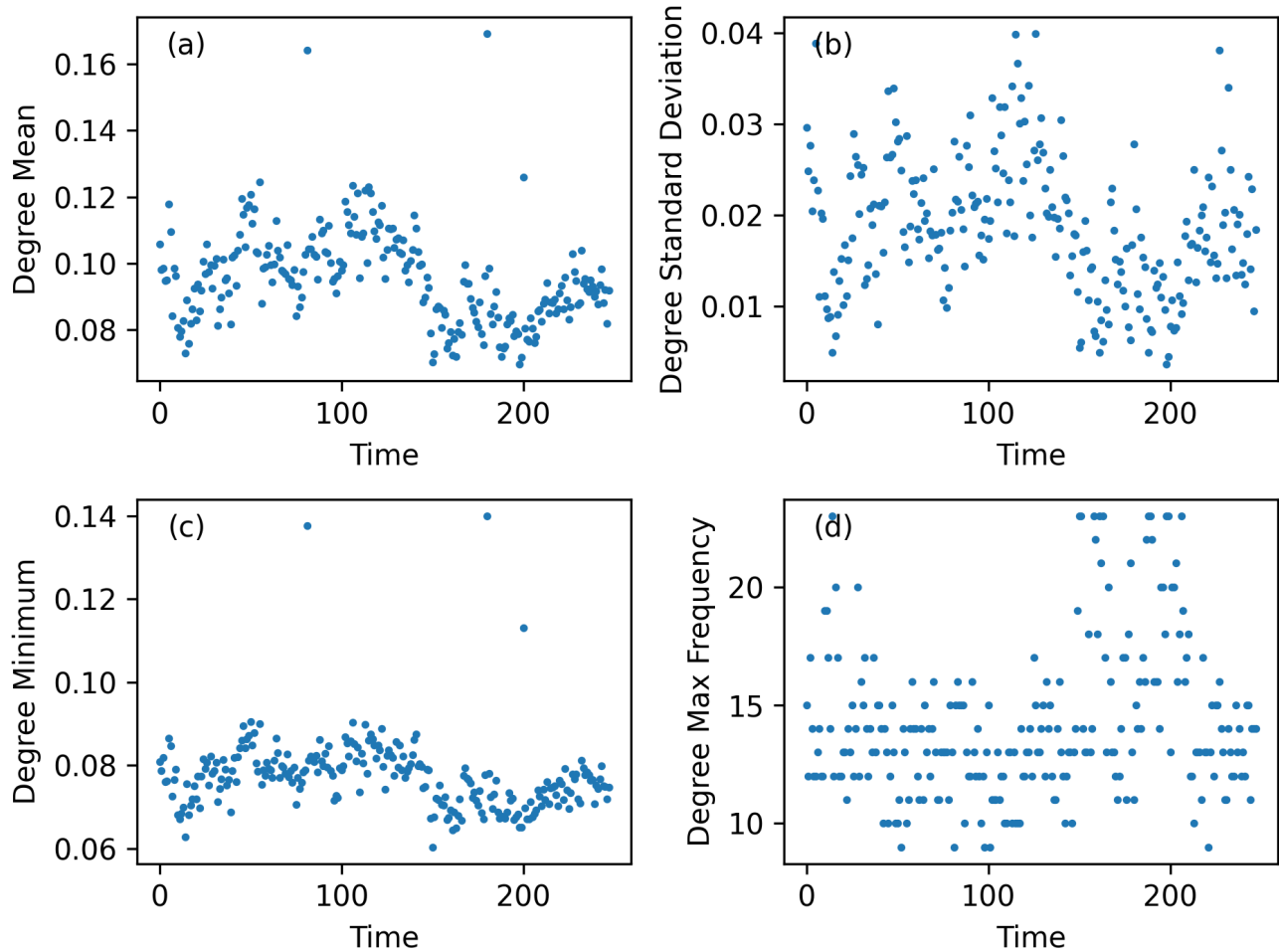


Figure 5: Evolution of Degree (a) Mean, (b) Standard Deviation, (c) Minimum and (d) Maximum.

presence of outlier days.

Let's say that if the normalized eigenvector centrality or degree vectors are understood to be measures of market direction and strength, by measuring which specific stocks are driving it and how much, their histograms, by disregarding the latter information, can be understood to measure just the intensity of this “market force”, how much stocks are well connected and so on.

## 6 Clustering Analysis

Next, we want to define a matrix distance  $\zeta(A, B)$  to measure similarity between networks. After inspection of similarity matrices with different metrics ( $L^1$ ,  $L^2$ , Jensen-Shannon Distance (the square root of  $D_{JS}$ )) and different phase representation (distances are measured between the whole transcript synchronization matrices, the EVC or

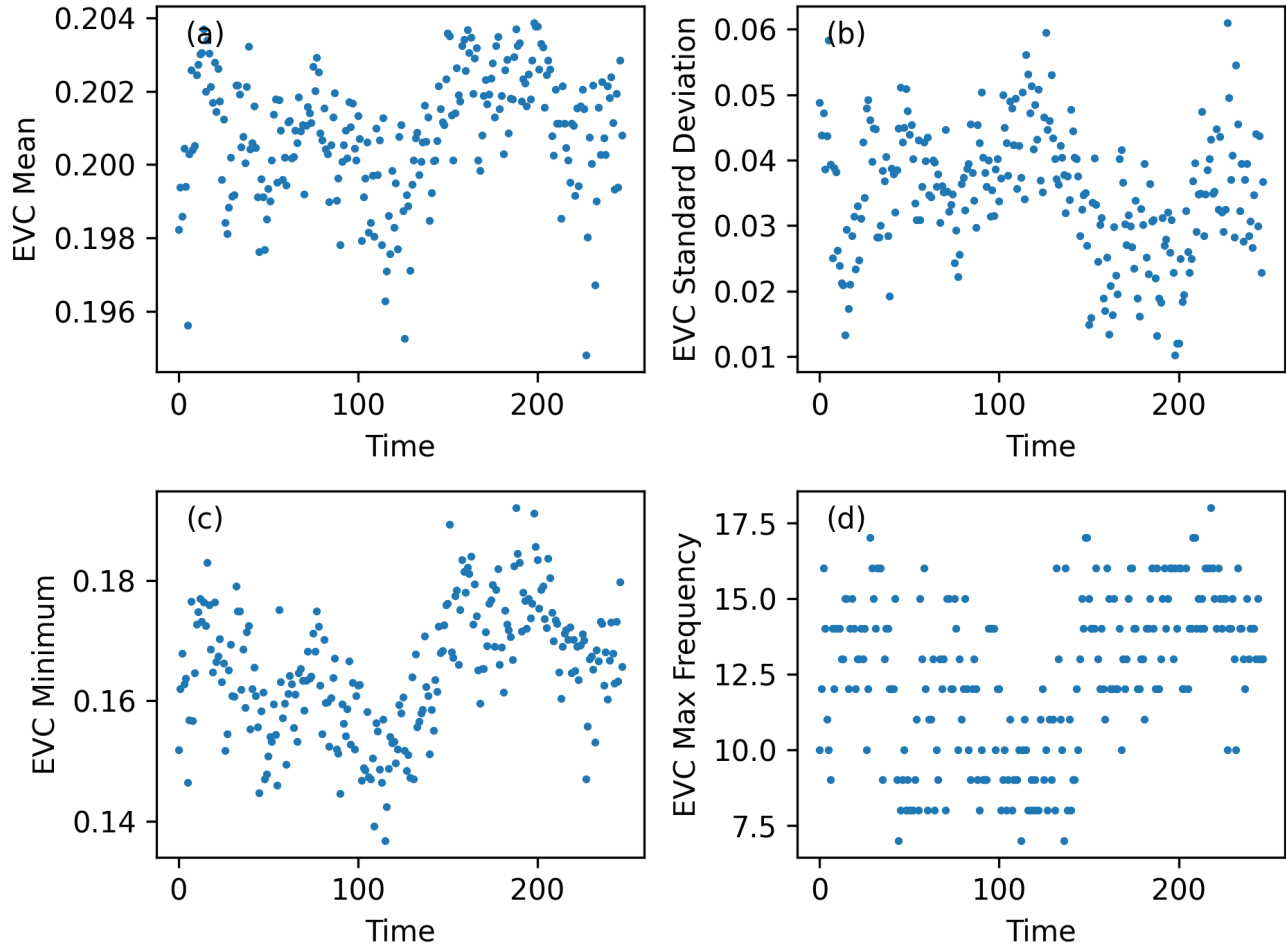


Figure 6: Evolution of Eigenvector Centrality (a) Mean, (b) Standard Deviation, (c) Minimum and (d) Maximum.

degree vectors, and also between their histograms) one can conclude that whether we use  $L^2$  or Jensen-Shannon Distance we arrive to similar results, and the difference lies in the phase representations, of which the histograms of degree or/and EVC seem to be the most informative ones. Thus, in what follows we will be studying not the adjacency matrices themselves, but the histograms of their EVC and Degree vectors. Since it is more meaningful than  $L^2$  norm when measuring distances between probability distributions (it can be understood as a minimum redundancy measure [51]), we will use the Jensen-Shannon distance for the dendrogram clustering. This is done also in order to reflect the previously founded structure.

If we then plot the Jensen-Shannon distance matrix  $D_{ij} = \zeta_{JS}(H_i^{transcript}, H_j^{transcript})$ , whose  $ij$  term equals the Jensen-Shannon distance between networks corresponding to days  $i$  and  $j$ , on Degree phase space (figure 8) we can clearly distinguish our outlier days as particularly distant of the typical days, which are very close to each other, thus confirming our previous idea: these days we observe a collective behavior in terms of determinism. In the same

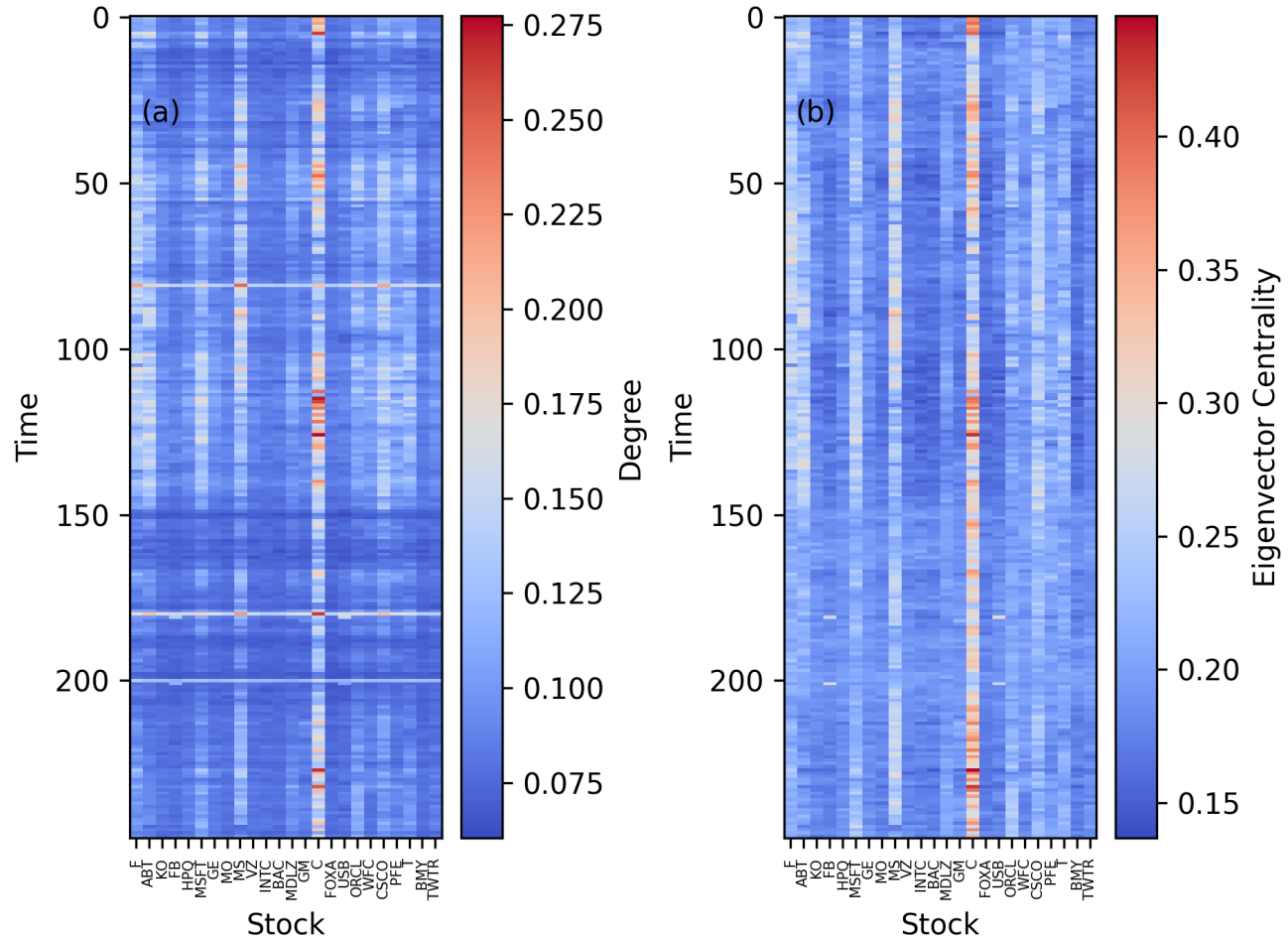


Figure 7: Evolution Through the Trading Year of (a) Degree and (b) Eigenvector Centrality per stock.

figure, as also in figure 9, which shows the same for EVC phase space, we observe at least two well separated seasons, previously identified as centralized and decentralized connectedness seasons. They exhibit oscillations but are clearly distinguishable by their internal coherence (low distances detected as blue blocks on diagonal) as well as the high distances between them (yellow strips in the figures).

While both phase spaces are good detecting structure in periods (highly decentralized season for instance), degree is far better highlighting outlier days.

Of course, to choose the phase space as that of the histograms is problematic in that it adds an extra, possibly very sensitive parameter, and more generally a whole new problem: the number of bins and the binning process. Here we choose ten uniformly sized bins covering the whole range of the corresponding quantity throughout the trading year.

We can now use  $\zeta$  to cluster our daily matrices (and thus our dynamical weighted network) looking for

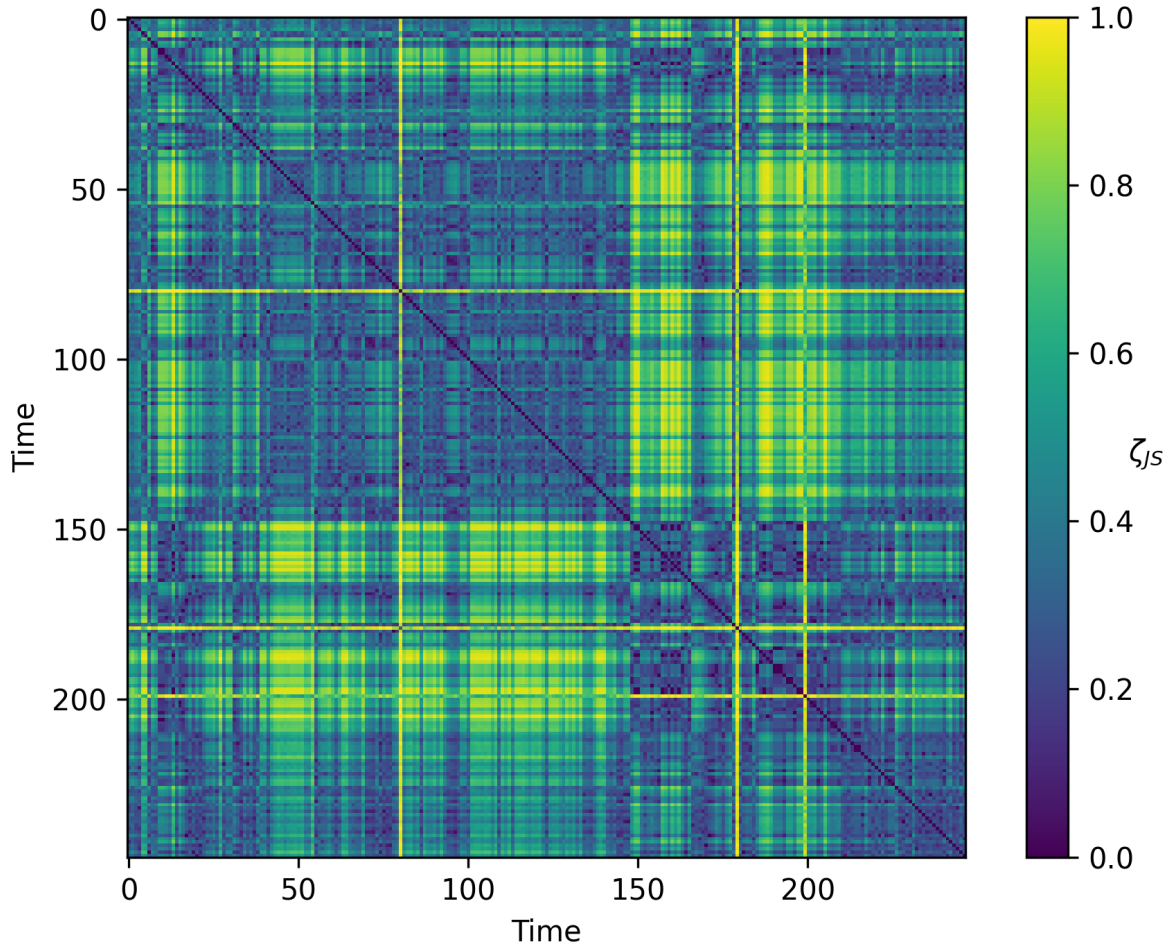


Figure 8: Jensen-Shannon Distance Matrix in Degree Phase Space. Its  $ij$  term equals the Jensen-Shannon distance between networks corresponding to days  $i$  and  $j$

distinctions between collective states [3] [4] [9][6]. For this, we use two very different algorithms: an agglomerative dendrogram with the Jensen-Shannon distance and a manually chosen cut-off threshold to stop the merging process (figures 10 and 11, the threshold is shown as an horizontal black line) and the  $L^2$ -based K-Means algorithm. As the dendrogram gives us lots of clusters with just a couple of elements as their members, we, in order to keep the number of clusters reasonable, merge all of those with 3 elements or less into a unique set labeled as “Noise”, yet at the cost of losing some information about outliers, which as we will see will be recovered by the K-Means algorithm. The other clusters, which are our states and after the last merge into the noise set turn out to be 12 for Degree and 14 for EVC, are ordered according to the Jensen-Shannon distance between the centroid (mean) of each of them and the corresponding uniform distributions, while the clusters obtained by the K-Means algorithm are ordered by their  $L^2$ -norm. The cophenetic correlation of the JS-based dendrograms are 0.41 for 0.43 for Degree and EVC phase spaces respectively. When applying K-Means algorithm, we choose the same number of clusters

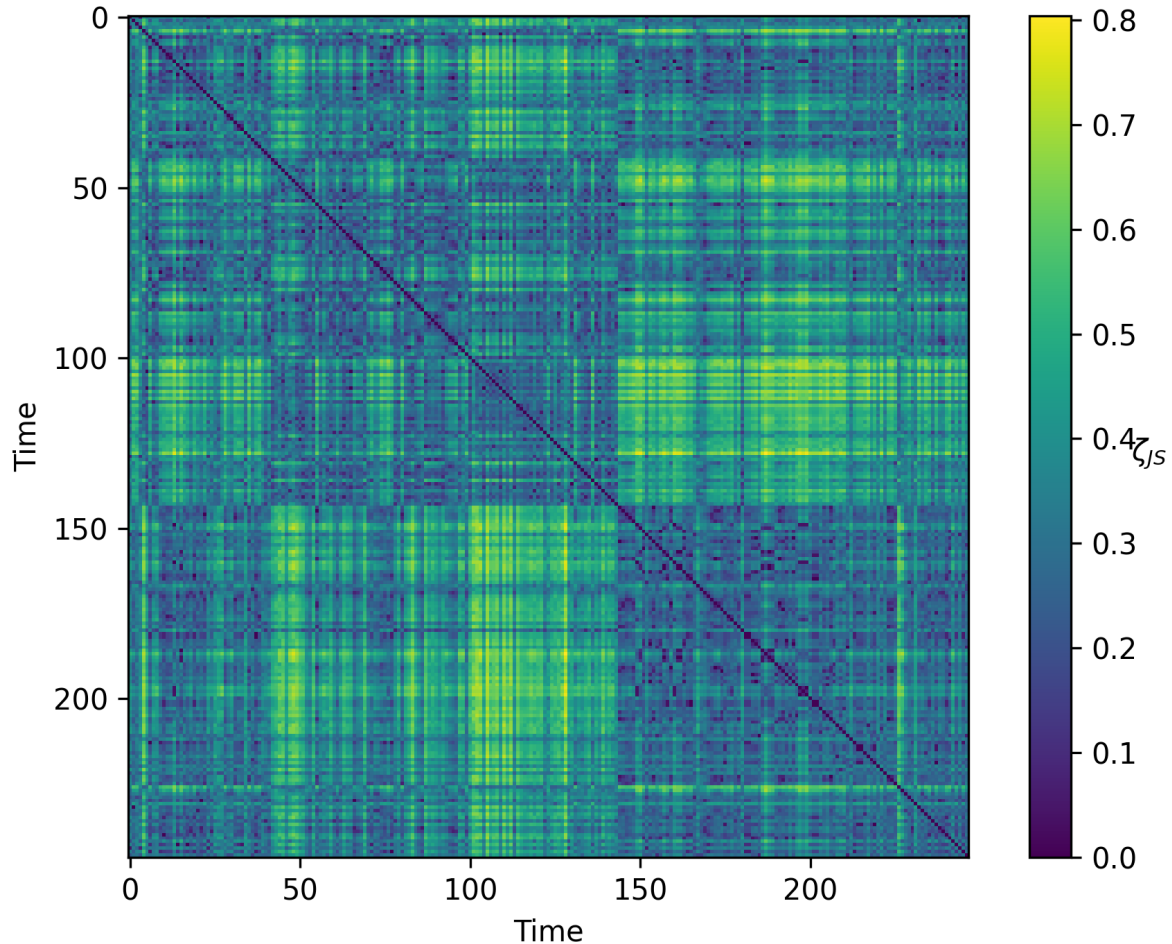


Figure 9: Jensen-Shannon Distance Matrix in EVC Phase Space. Its  $ij$  term equals the Jensen-Shannon distance between networks corresponding to days  $i$  and  $j$

as that obtained by the dendrogram algorithm.

In the next figures, the upper panel displays the evolution of states throughout the year (noise days are plotted as black, smaller dots at the bottom of the graph when dendrogram is used) and the lower displays the  $\zeta_{JS}$  or  $L^2$ -ordered centroids of the clusters (states). While both clustering methods agree in the detection of a low-states season and a high-states one, as well as in the shape of the centroids (of non-singleton clusters), they display different, complementary features.

First of all, it is noteworthy that both phase spaces and with both clustering methods, very different in nature and using two different distances, display very similar dynamics (figures 12- 15). This is a strong feature supporting our findings, as we can observe the highly decentralized season with particular persistence and clarity, as well as roughly monthly oscillations, less clear for dendrogram algorithm due to the way we labeled days as noisy.

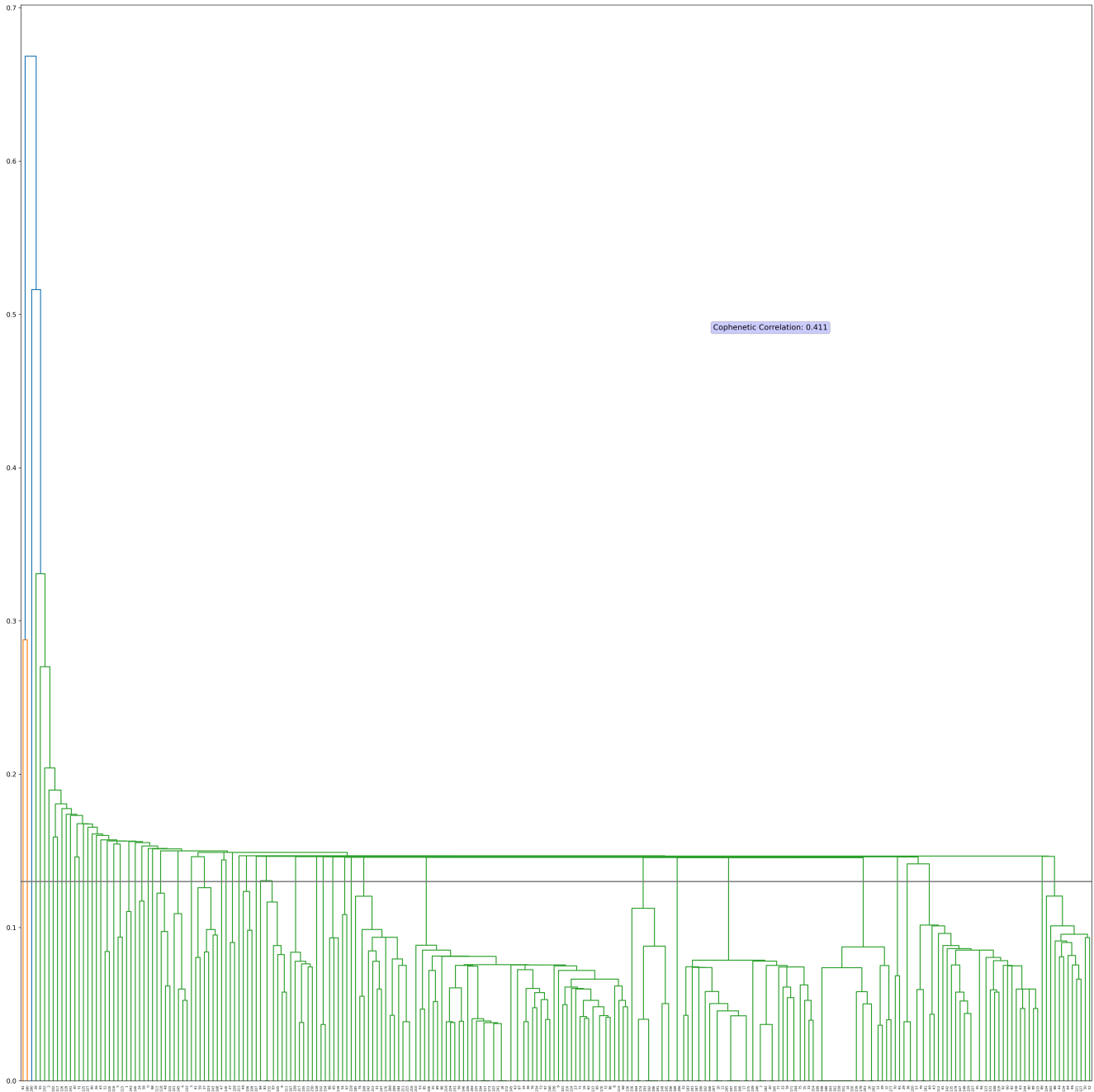


Figure 10: Clustering Dendrogram on Degree Phase Space with Jensen-Shannon Distance.

Note that the K-Means algorithm gives us extra information about the outlier days: the first two belong to exceptionally low states, while the last outlier day belongs to one of the highest and most Dirac-like clusters, so it is of a different nature, a decentralized one.

In figures 16 and 17 we visualize the same information in a different way, by plotting the same histograms as in figures 4 but this time colored according to their founded clusters-states.

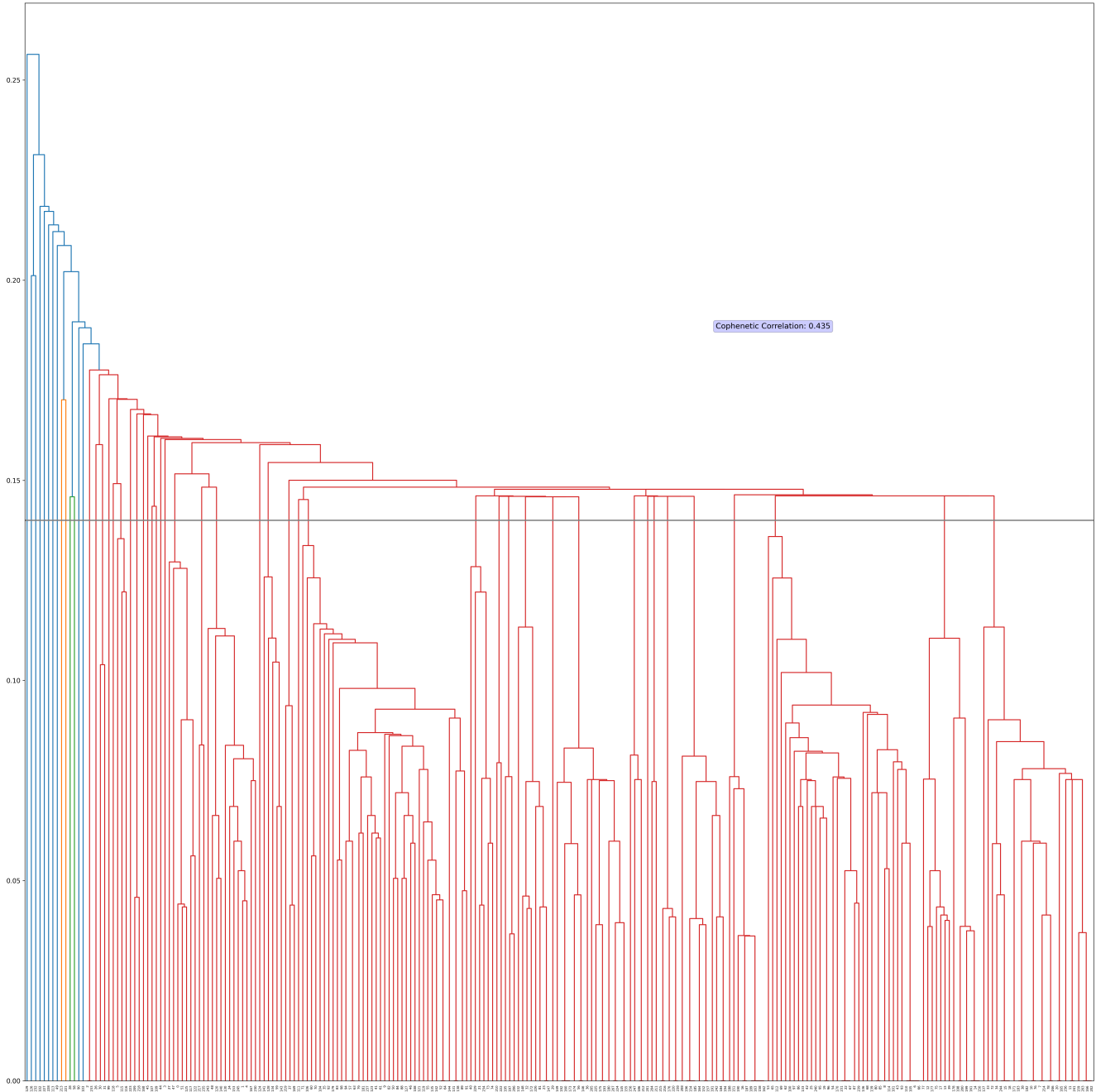


Figure 11: Clustering Dendrogram on EVC Phase Space with Jensen-Shannon Distance.

## 7 A Markov Model for State Transitions

In order to model these state dynamics in a simple way, we propose a first order Markov model for prediction of the next day state given that we know today market state. First, let's visualize first order transition probabilities.

The left panel in figures 18- 21 shows the empirical transition probability matrix  $P$  from one state to the next,

given that we know the current state, while the right panel shows the same information in graph form, with states as nodes and transition probabilities as edge weights. For a better visualization we plot only the edges whose weight is greater than  $1/n_{clusters}$ , where  $n_{clusters}$  is the number of clusters or typical states, that is, we plot just those transition edges which are more likely to be observed than a random guess transition. Also, edge widths are proportional to weights and node sizes are proportional to the absolute frequency of each state.

The transition matrices show high values mainly near their diagonals, which means that jumps from one state to another are likely to happen only if they are close states. This means that low or high states regimes are persistent. In some cases this is not too much information: for example, in figure 20 we can see from the transition matrix that, given that we are in market state 2, we are pretty sure that the next state will be 0; but the thing is, we almost never observe the market in state 2 as we see in the size of the corresponding node in the graph, so that's not really a transition we should expect to find. On the contrary, from figure 21 we know that if we observe today market state 10, there is a high probability that the next state will be 10 or 8, and we also know from the graph that those are two very likely transitions to observe, since the market spends many days in those states as indicated by their node sizes.

To check whether this markovian approach is adequate or not we, just as in [9], compute the theoretical stationary probability distribution of states for such a Markov model given by the first order transition matrix  $P$ , that is, the probability distribution  $\pi$  giving the expected probabilities of finding the market in a given state over a very long period (provided it is markovian), and satisfying the linear equation:

$$\pi_j = \sum_i P_{ij}\pi_i,$$

and compare it to the empirical frequencies of states through the year (figure 22), just to find that they are indeed very similar to each other for every combination of phase spaces and clustering algorithms. We then conclude that, as pointed out before, to guess tomorrow state given knowledge about today state is in general a reasonable bet.

A considerable part of our work on ordinal patterns has been done with the Python package `ordpy` [52], while clustering analysis has been carried out through `scikit-learn` [53]. We also have made extensive, though elementary, use of `NumPy` [54].

## 8 Conclusions

In order to analyze collective states dynamics of stocks in high-frequency digital markets, and to overcome the limitations of correlation matrices in detecting non-linear interactions in noisy time series, we proposed to study transcripts synchronization dynamical networks and their eigenvector centrality and degree vectors distributions.

After measuring different information theoretic quantities on the daily ordinal pattern series of individual stocks and founding some features as outlier behavior of some days in most of them and discrete levels in some, we have

shown them to be extreme manifestations of a collective, emergent behavior not entirely reflected in individual dynamics. Applying two very different clustering algorithms, we were able to detect specific, persistent and quantitatively distinguishable market states throughout the one-year period of study, as well as two well defined and quantitatively distinguishable seasons of the trading year, characterized by their degree of centralized/decentralized synchronicity, with remarkable similar results for both algorithms. Finally, we showed that state transitions dynamics can be well described as a simple first order Markov process.

Of course, our work has several limitations that ought to be highlighted. As already mentioned, to choose the phase space as that of the histograms of EVC and Degree leaves open the question of the correct number of bins to be used. Also, it would be desirable to find a more objective criterion to choose the number of clusters; various purely quantitative ones are discussed in the literature (see for a summary [55]), but none of those are convincing from our viewpoint; and ultimately, as explained in [56], clustering analysis is a problem dependent process and should not be subordinated to an abstract, global score. As our aim in this work was to propose and illustrate a methodology, as well as to adapt the network-clustering pipeline often mentioned throughout this work [6] to high-frequency digital markets, we did not deepen into this questions; instead, in both cases we contented ourselves with confirming the robustness of our results by varying the number of bins and dendogram threshold and founding similar qualitative results in a reasonable range of values and with two very different clustering algorithms for our particular data set.

## **Author Contributions**

Conceptualization, M.L.; methodology, M.L. and R.M.; software, M.L.; formal analysis, M.L.; investigation, M.L.; resources, R.M.; data curation, M.L. and R.M.; writing—original draft preparation, M.L.; writing—review and editing, M.L. and R.M.; visualization, M.L.; supervision, M.L. and R.M. All authors have read and agreed to the published version of the manuscript.

## **Funding**

This research received no external funding

## **Data Availability**

The data presented in this study are available [57].

## Conflicts of Interest

The authors declare no conflict of interest.

## References

- [1] Mantegna, R. N. Hierarchical structure in financial markets. *Eur. Phys. J. B* **1999**, *11*, 193–197. <https://doi.org/10.1007/s100510050929>.
- [2] Onnela, J.-P.; Chakraborti, A.; Kaski, K.; Kertész, J.; Dynamic asset trees and Black Monday. *Physica A* **2003**, *324*, 247–252. [https://doi.org/10.1016/s0378-4371\(02\)01882-4](https://doi.org/10.1016/s0378-4371(02)01882-4).
- [3] Marsili, M. Dissecting financial markets: Sectors and States. *Quant. Finance* **2002**, *2*, 297–302. <https://doi.org/10.1088/1469-7688/2/4/305>.
- [4] Münnix, M. C.; Shimada, T.; Schäfer, R.; Leyvraz, F.; Seligman, T. H.; Guhr, T.; Stanley, H. E. Identifying States of a Financial Market. *Sci. Rep.* **2012**, *2*. <https://doi.org/10.1038/srep00644>.
- [5] Chetalova, D.; Schäfer, R.; Guhr, T. Zooming into market states. *J. Stat. Mech.* **2015**, *1*, P01029. <https://doi.org/10.1088/1742-5468/2015/01/p01029>.
- [6] Masuda, N.; Holme, P. Detecting sequences of system states in temporal networks. *Sci. Rep.* **2019**, *9*, 795. <https://doi.org/10.1038/s41598-018-37534-2>.
- [7] Chakraborti, A.; Hrishidev; Sharma, K.; Pharasi, H. K. Phase separation and scaling in correlation structures of financial markets. *J. Phys. Complex.* **2021**, *2*, 015002. <https://doi.org/10.1088/2632-072X/abbed1>.
- [8] Chakraborti, A.; Sharma, K.; Pharasi, H. K.; Shuvo Bakar, K.; Das, S.; Seligman, T. H. Emerging spectra characterization of catastrophic instabilities in complex systems. *New J. Phys.* **2020**, *22*, 063043. <https://doi.org/10.1088/1367-2630/ab90d4>.
- [9] Pharasi, H. K.; Sharma, K.; Chatterjee, R.; Chakraborti, A.; Leyvraz, F.; Seligman, T. H. Identifying long-term precursors of financial market crashes using correlation patterns. *New J. Phys.* **2018**, *20*, 103041. <https://doi.org/10.1088/1367-2630/aae7e0>.
- [10] Musciotto, F.; Piilo, J.; Mantegna, R. N. High-frequency trading and networked markets. *Proc. Natl. Acad. Sci. U.S.A.*, **2021**, *118*, e2015573118. <https://doi.org/10.1073/pnas.2015573118>.
- [11] Kim, M.; Sayama, H. Predicting stock market movements using network science: an information theoretic approach. *Appl. Netw. Sci.* **2017**, *2*. <https://doi.org/10.1007/s41109-017-0055-y>.

- [12] Zanin, M.; Zunino, L.; Rosso, O. A.; Papo, D. Permutation Entropy and Its Main Biomedical and Econophysics Applications: A Review. *Entropy* **2012**, *14*, 1553–1577. <https://doi.org/10.3390/e14081553>.
- [13] Bandt, Ch.; Pompe, B. Permutation Entropy: A Natural Complexity Measure for Time Series. *Phys. Rev. Lett.* **2002**, *88*, 174102-1 – 174102-4. <https://doi.org/10.1103/PhysRevLett.88.174102>.
- [14] Cysarz, D.; Van Leeuwen, P.; Edelhauser, F.; Montano, N.; Porta, A. Binary symbolic dynamics classifies heart rate variability patterns linked to autonomic modulations. *Comput. Biol. Med.* **2012**, *42*, 313–318. <https://doi.org/10.1016/j.compbiomed.2011.04.013>.
- [15] Parlitz, U.; Berg, S.; Luther, S.; Schirdewan, A.; Kurths, J.; Wessel, N. Classifying cardiac biosignals using ordinal pattern statistics and symbolic dynamics. *Comput. Biol. Med.* **2012**, *42*, pp. 319–27. <https://doi.org/10.1016/j.compbiomed.2011.03.017>.
- [16] Nicolaou, N.; Georgiou, J. Detection of epileptic electroencephalogram based on Permutation Entropy and Support Vector Machines. *Expert Syst. Appl.* **2012**, *39*, 202–209. <https://doi.org/10.1016/j.eswa.2011.07.008>.
- [17] Ouyang, G.; Li, X.; Dang, C.; Richards, D. A. Deterministic dynamics of neural activity during absence seizures in rats. *Phys. Rev. E* **2009**, *79*, 041146. <https://doi.org/10.1103/physreve.79.041146>.
- [18] Faes, L.; Nollo, G.; Porta, A. Non-uniform multivariate embedding to assess the information transfer in cardiovascular and cardiorespiratory variability series. *Comput. Biol. Med.* **2010**, *42*, 290–297. <https://doi.org/10.1016/j.compbiomed.2011.02.007>.
- [19] Bian, C.; Qin, C.; Ma, Q. D. Y.; Shen, Q. Modified permutation-entropy analysis of heartbeat dynamics. *Phys. Rev. E* **2012** *85*, 021906. <https://doi.org/10.1103/physreve.85.021906>.
- [20] Li, X.; Ouyang, G. Estimating coupling direction between neuronal populations with permutation conditional mutual information. *NeuroImage* **2010**, *52*, 497–507. <https://doi.org/10.1016/j.neuroimage.2010.05.003>.
- [21] Olofsen, E.; Sleigh, J. W.; Dahan, A. Permutation entropy of the electroencephalogram: a measure of anaesthetic drug effect. *Br. J. Anaesth.* **2008**, *101*, 810–821. <https://doi.org/10.1093/bja/aen290>.
- [22] Garland, J.; Jones, T. R.; Neuder, M.; Morris, V.; White, J. W. C.; Bradley, E. Anomaly Detection in Paleoclimate Records using Permutation Entropy. *Entropy* **2018**, *20*, 931. <https://doi.org/10.3390/e20120931>.
- [23] Ruiz, M. C.; Guillamón, A.; Gabaldón, A. A New Approach to Measure Volatility in Energy Markets. *Entropy* **2012**, *14*, 74–91. <https://doi.org/10.3390/e14010074>.

- [24] Zanin, M. Forbidden patterns in financial time series. *Chaos* **2008**, *18*, 013119. <https://doi.org/10.1063/1.2841197>
- [25] Zunino, L.; Zanin, M.; Tabak, B. M.; Pérez, D. G.; Rosso, O. A. Forbidden patterns, permutation entropy and stock market inefficiency. *Physica A* **2009**, *388*, 2854–2864. <https://doi.org/10.1016/j.physa.2009.03.042>.
- [26] Zunino, L.; Zanin, M.; Tabak, B. M.; Pérez, D. G.; Rosso, O. A. Complexity-entropy causality plane: A useful approach to quantify the stock market inefficiency. *Physica A* **2010**, *389*, 1891–1901. <https://doi.org/10.1016/j.physa.2010.01.007>.
- [27] Zunino, L.; Fernández Bariviera, A.; Guercio, M. B.; Martinez, L. B.; Rosso, O. A. On the efficiency of sovereign bond markets. *Physica A* **2012**, *391*, 4342–4349. <https://doi.org/10.1016/j.physa.2012.04.009>.
- [28] Zunino, L.; Tabak, B. M.; Serinaldi, F.; Zanin, M.; Pérez, D. G.; Rosso, O. A. Commodity predictability analysis with a permutation information theory approach. *Physica A* **2011**, *390*, 876–890. <https://doi.org/10.1016/j.physa.2010.11.020>.
- [29] Pessa, A. A. B.; Ribeiro, H. V.; Characterizing stochastic time series with ordinal networks. *Phys. Rev. E* **2019**, *100*, 042304. <https://doi.org/10.1103/physreve.100.042304>.
- [30] Yan, R.; Liu, Y.; Gao, R. X. Permutation entropy: A nonlinear statistical measure for status characterization of rotary machines. *Mech. Syst. Signal Process.* *2012*, *29*, 474–484. <https://doi.org/10.1016/j.ymssp.2011.11.022>.
- [31] Fadlallah, B.; Chen, B.; Keil, A.; Príncipe, J. Weighted-permutation entropy: A complexity measure for time series incorporating amplitude information. *Phys. Rev. E* **2013**, *87*, 022911 – 022911. <https://doi.org/10.1103/PhysRevE.87.022911>.
- [32] Liu, X.; Wang, Y. Fine-grained permutation entropy as a measure of natural complexity for time series. *Chin. Phys. B* **2009**, *18*, 2690. <https://doi.org/10.1088/1674-1056/18/7/011>.
- [33] Staniek, M.; Lehnertz, K. Symbolic Transfer Entropy. *Phys. Rev. Lett.* **2008**, *100*, 158101. <https://doi.org/10.1103/physrevlett.100.158101>.
- [34] Amigó, J. M.; Monetti, R.; Graff, B.; Graff, G. Computing algebraic transfer entropy and coupling directions via transcripts. *Chaos* **2016**, *26*, 113115. <https://doi.org/10.1063/1.4967803>.
- [35] López-Ruiz, R.; Mancini, H. L.; Calbet, X. A statistical measure of complexity. *Phys. Lett. A* **1995**, *209*, 321–326. doi:10.1016/0375-9601(95)00867-5

- [36] Lamberti, P.; Martin, M.; Plastino, A.; Rosso, O. Intensive entropic non-triviality measure. *Physica A* **2004**, *334*, 119-131. <https://doi.org/10.1016/j.physa.2003.11.005>.
- [37] Bahraminasab, A.; Ghasemi, F.; Stefanovska, A.; McClintock, P. V. E.; Kantz, H. Direction of Coupling from Phases of Interacting Oscillators: A Permutation Information Approach. *Phys. Rev. Lett.* **2008**, *100*, 084101. <https://doi.org/10.1103/physrevlett.100.084101>.
- [38] Monetti, R.; Bunk, W.; Aschenbrenner, T.; Jamitzky, F. Characterizing synchronization in time series using information measures extracted from symbolic representations. *Phys. Rev. E* **2009**, *79*. <https://doi.org/10.1103/physreve.79.046207>.
- [39] Keller, K.; Mangold, T.; Stolz, I.; Werner, J. Permutation Entropy: New Ideas and Challenges. *Entropy* **2017**, *19*, 134. <https://doi.org/10.3390/e19030134>.
- [40] Amigó, J. M.; Monetti, R.; Aschenbrenner, T.; Bunk, W. Transcripts: An algebraic approach to coupled time series. *Chaos* **2012**, *22*, 013105. <https://doi.org/10.1063/1.3673238>.
- [41] Bunk, W.; Amigó, J. M.; Aschenbrenner, T.; Monetti, R. A new perspective on transcripts by means of their matrix representation. *Eur. Phys. J. Special Top.* **2013**, *222*, 363–381. <https://doi.org/10.1140/epjst/e2013-01847-6>.
- [42] Zunino, L.; Olivares, F.; Scholkmann, F.; Rosso, O. A. Permutation entropy based time series analysis: Equalities in the input signal can lead to false conclusions. *Phys. Lett. A* **2017**, *381*, 1883–1892. <https://doi.org/10.1016/j.physleta.2017.03.052>.
- [43] Quintero-Quiroz, C.; Pigolotti, S.; Torrent, M. C.; Masoller, C. Numerical and experimental study of the effects of noise on the permutation entropy. *New J. Phys.* **2015**, *17*, 093002. <https://doi.org/10.1088/1367-2630/17/9/093002>.
- [44] Amigó, J. M.; Zambrano, S.; Sanjuán, M. A. F. True and false forbidden patterns in deterministic and random dynamics. *Europhys. Lett.* **2007**, *79*, 50001. <https://doi.org/10.1209/0295-5075/79/50001>.
- [45] McCullough, M.; Small, M.; Iu, H. H. C.; Stemler, T. Multiscale ordinal network analysis of human cardiac dynamics. *Philos. Trans. R. Soc. A* **2017**, *375*, 20160292. <https://doi.org/10.1098/rsta.2016.0292>.
- [46] Campanharo, A. S. L. O.; Sirer, M. I.; Malmgren, R. D.; Ramos, F. M.; Amaral, L. A. N. Duality between Time Series and Networks. *PLoS ONE* **2011**, *6*, e23378. <https://doi.org/10.1371/journal.pone.0023378>.
- [47] Zhang, J.; Zhou, J.; Tang, M.; Guo, H.; Small, M.; Zou, Y. Constructing ordinal partition transition networks from multivariate time series. *Sci. Rep.* **2017**, *7*, 7795. <https://doi.org/10.1038/s41598-017-08245-x>.

- [48] Olivares, F.; Zanin, M.; Zunino, L.; Pérez, D. G. Contrasting chaotic with stochastic dynamics via ordinal transition networks. *Chaos* **2020**, *30*, 063101. <https://doi.org/10.1063/1.5142500>.
- [49] Matilla-García, M.; Ruiz Marín, M. A non-parametric independence test using permutation entropy. *J. Econom.* **2008**, *144*, 139–155. <https://doi.org/10.1016/j.jeconom.2007.12.005>.
- [50] Monetti, R.; Bunk, W.; Aschenbrenner, T.; Springer, S.; Amigó, J. M. Information directionality in coupled time series using transcripts. *Phys. Rev. E* **2013**, *88*. <https://doi.org/10.1103/physreve.88.022911>.
- [51] Endres, D. M.; Schindelin, J. E. A new metric for probability distributions. *IEEE Trans. Inf. Theory* **2003**, *49*, 1858–1860. <https://doi.org/10.1109/tit.2003.813506>.
- [52] Pessa, A. A. B.; Ribeiro, H. V. ordpy: A Python package for data analysis with permutation entropy and ordinal network methods. *Chaos* **2021**, *31*, 063110. <https://doi.org/10.1063/5.0049901>.
- [53] Pedregosa, F.; Varoquaux, G.; Gramfort, A.; Michel, V.; Thirion, B.; Grisel, O.; Blondel, M.; Prettenhofer, P.; Weiss, R.; Dubourg, V.; Vanderplas, J.; Passos, A. Cournapeau, D.; Brucher, M.; Perrot, M.; Duchesnay, E. Scikit-learn: Machine Learning in Python. *J. Mach. Learn. Res.* **2011**, *12*, 2825–2830. <http://jmlr.org/papers/v12/pedregosa11a.html>.
- [54] Harris, C.R.; Millman, K.J.; van der Walt, S.J. et al. Array programming with NumPy. *Nature* **2020**, *585*, 357–362. <https://doi.org/10.1038/s41586-020-2649-2>.
- [55] Arbelaitz, O.; Gurrutxaga, I.; Muguerza, J.; Pérez, J. M.; Perona, I. An extensive comparative study of cluster validity indices. *Pattern Recognit.* **2013**, *46*, 243–256. <https://doi.org/10.1016/j.patcog.2012.07.021>.
- [56] von Luxburg, U.; Williamson, R. C.; Guyon, I. Clustering: science or art?. In Proceedings of ICML Workshop on Unsupervised and Transfer Learning, Bellevue, Washington, USA, 2 July 2011; Guyon, I., Dror, G., Lemaire, V, Taylor, G., Silver, D., Eds.
- [57] Ordinal Synchronization Repository. Available online: <https://gitlab.com/mario-lopez-perez/ordinal-synchronization> (accessed on October 2th, 2021).

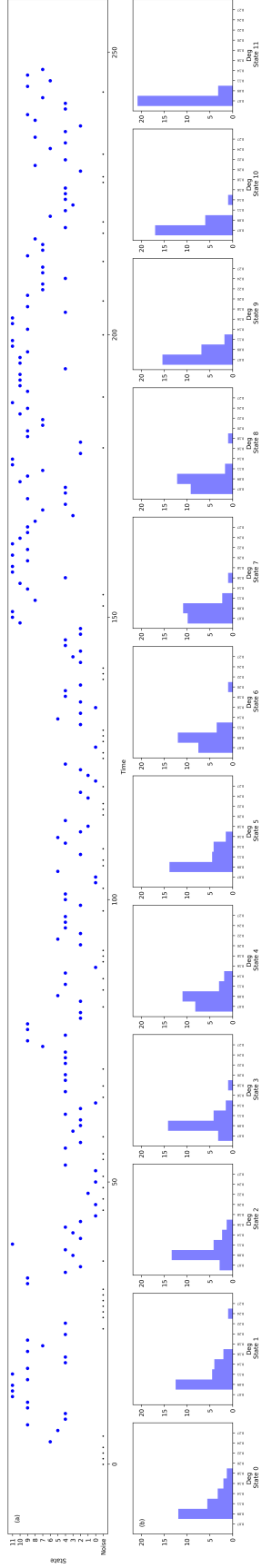


Figure 12: (a) Evolution of States in Degree Phase Space and (b)  $\zeta_S$ -ordered Centroids, Dendrogram Algorithm.

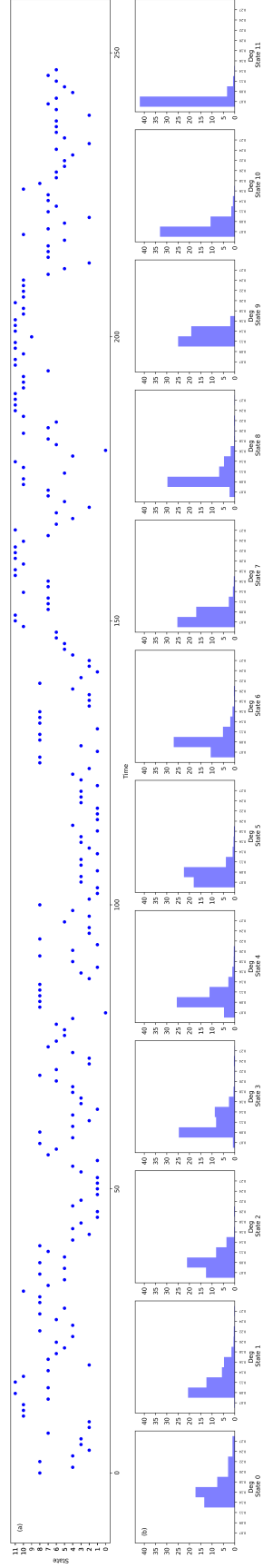


Figure 13: (a) Evolution of States in Degree Phase Space and (b)  $L^2$ -ordered Centroids, K-Means Algorithm.

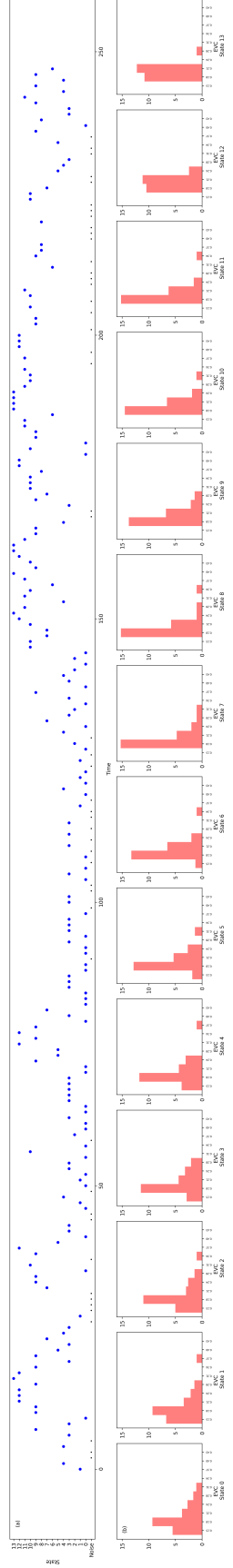


Figure 14: (a) Evolution of States in EVC Phase Space and (b)  $\zeta_{IS}$ -ordered Centroids, Dendrogram Algorithm.

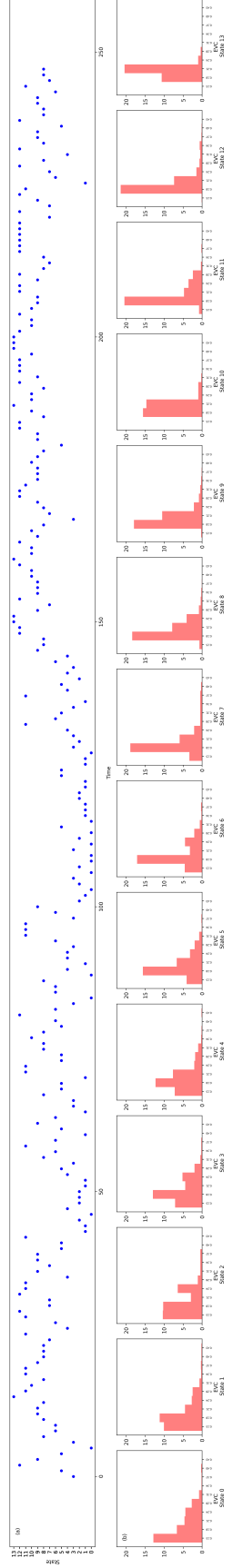


Figure 15: (a) Evolution of States in EVC Phase Space and (b)  $L^2$ -ordered Centroids, K-Means Algorithm.

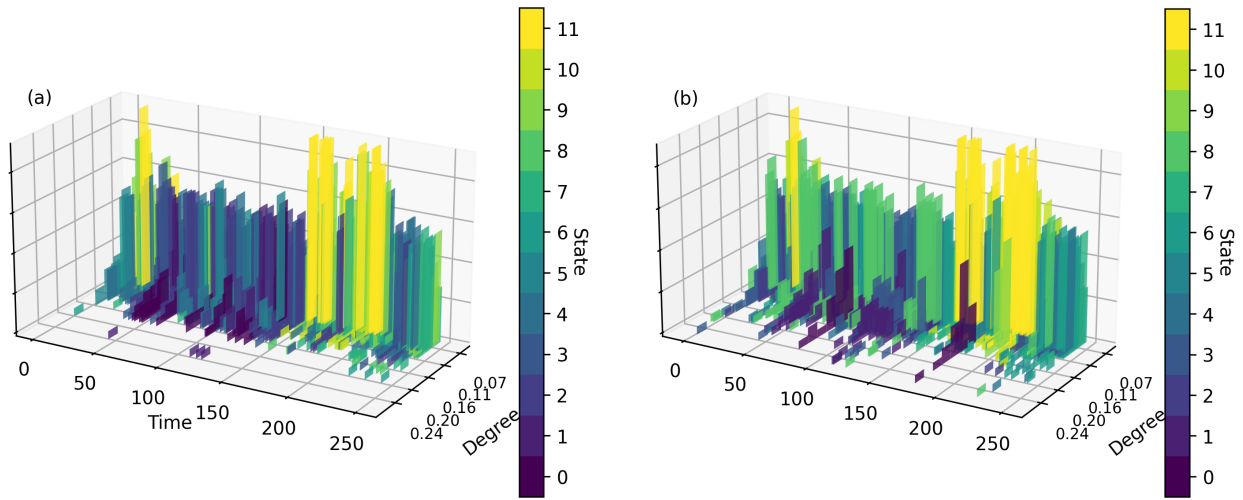


Figure 16: Evolution of Histogram of Degree Colored by State. (a) Dendrogram, (b) K-Means algorithm.

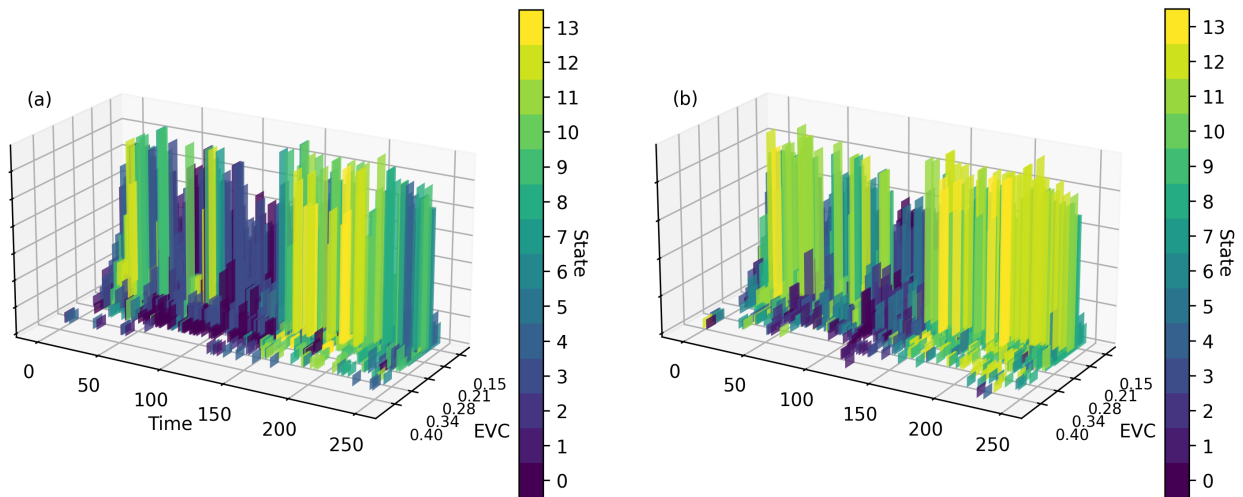


Figure 17: Evolution of Histogram of EVC Colored by State. (a) Dendrogram, (b) K-Means algorithm.

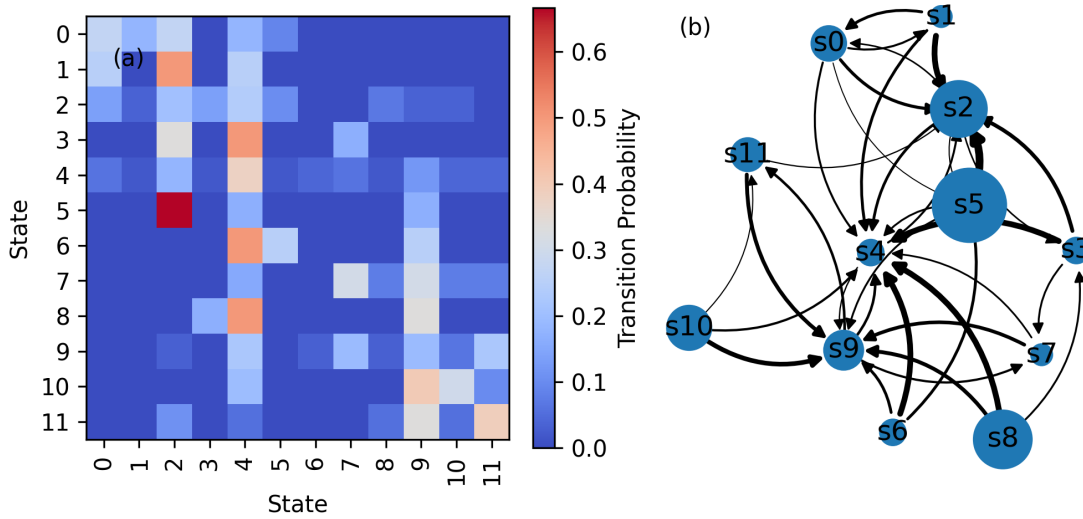


Figure 18: Transition Probabilities from One State to the Next in Degree Phase Space with Dendrogram Algorithm. (a) Transition Probability Matrix, (b) Transition Directed Network

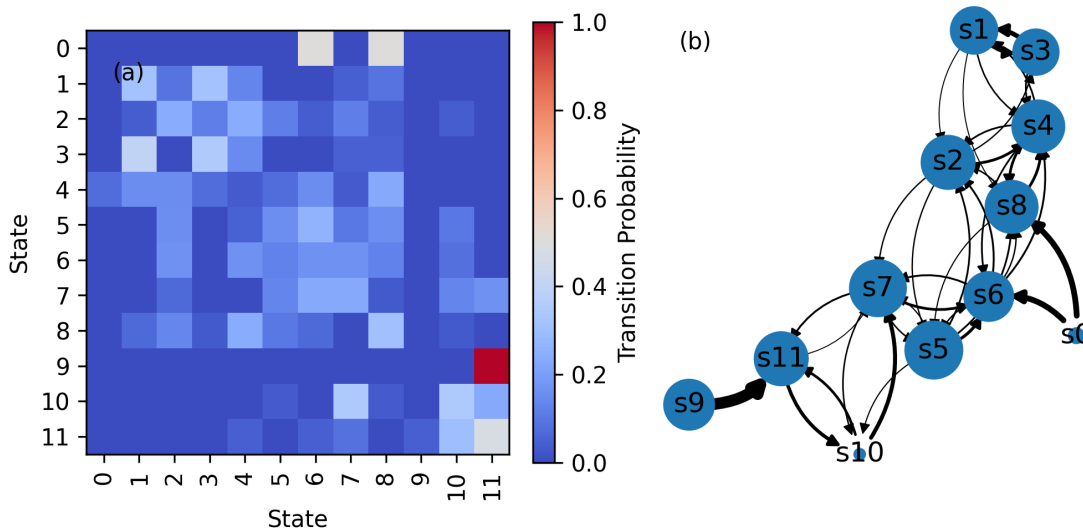


Figure 19: Transition Probabilities from One State to the Next in Degree Phase Space with K-Means Algorithm. (a) Transition Probability Matrix, (b) Transition Directed Network

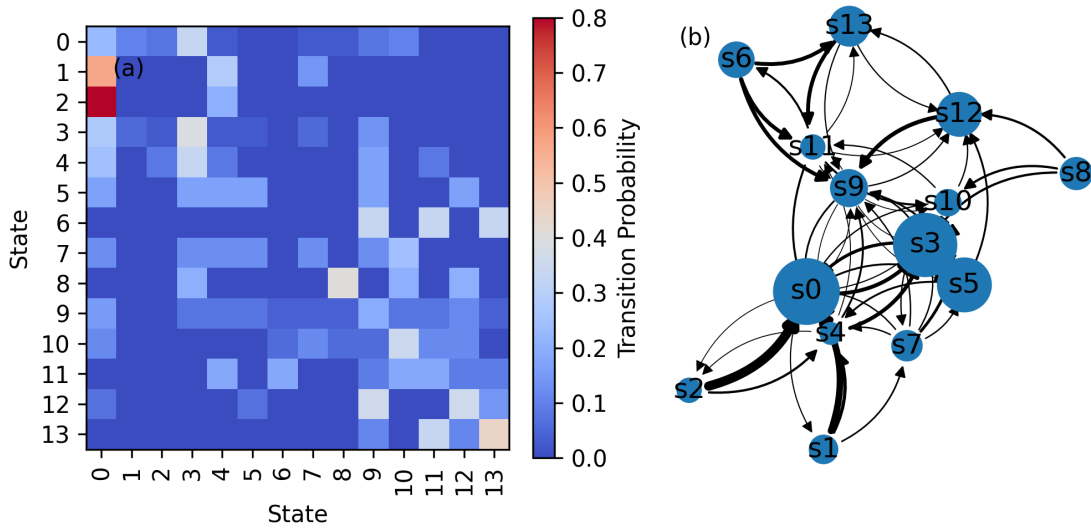


Figure 20: Transition Probabilities from One State to the Next in EVC Phase Space with Dendrogram Algorithm. (a) Transition Probability Matrix, (b) Transition Directed Network

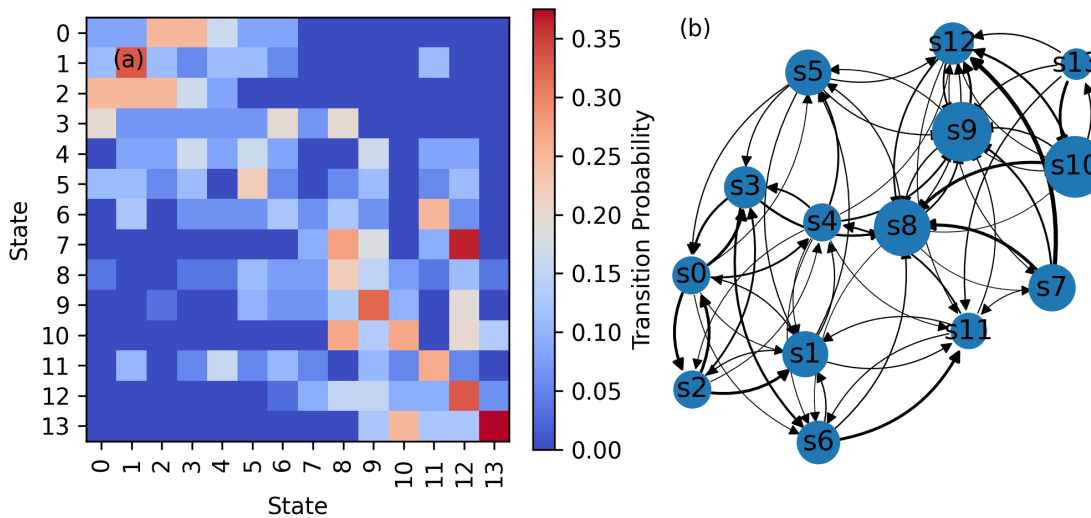


Figure 21: Transition Probabilities from One State to the Next in EVC Phase Space with K-Means Algorithm. (a) Transition Probability Matrix, (b) Transition Directed Network

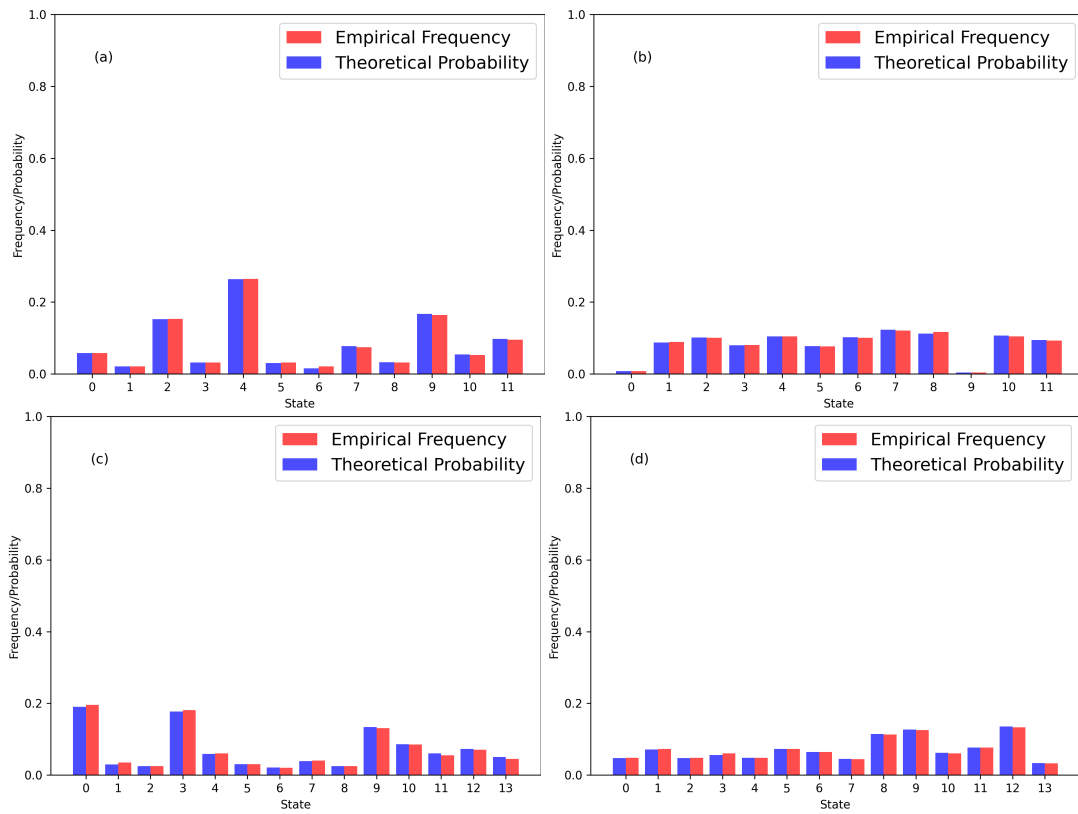


Figure 22: Empirical Frequency of States and Theoretical Stationary Distribution for the Markov Model.  
 (a) Degree, Dendrogram; (b) Degree, K-Means; (c) EVC, Dendrogram; (d) EVC, K-Means.